

ADVANCES IN PRECISION POINTING CONTROL FOR THE NASA SPITZER SPACE TELESCOPE

David S. Bayard ¹

This paper discusses the pointing control system for NASA's Space Infra-Red Telescope Facility (SIRTF). SIRTF was launched in August 2003, and was commissioned in December 2003 as the Spitzer Space Telescope. SIRTF represents the last spacecraft in NASA's Great Observatory series. In general, space telescopes present a major challenge for precision pointing control. The SIRTF pointing control system achieves arcsecond-level pointing accuracy and sub-arcsecond pointing jitter while supporting a broad range of payload instrument requirements and science observing modes. SIRTF carries three science payload instruments: the Infrared Array Camera (IRAC), the Infrared Spectrograph (IRS) and the Multi-band Imaging Photometer for SIRTF (MIPS). Each science instrument brings its own unique set of constraints and challenges for the pointing control system design. After an introduction to the SIRTF mission, telescope and science instruments, an overview is given of the SIRTF pointing control system. Discussion is focused on the pointing control hardware, architecture, pointing requirements/capability, attitude constraints/commanding, attitude observers, and required calibrations. Advances and novel aspects of the pointing system design are emphasized.

INTRODUCTION

SIRTF is an infrared space telescope which is the last in NASA's Great Observatory series. This well-known series includes the Hubble Space Telescope for the visible frequencies, AXAF (Chandra) for X-ray, and the Compton Gamma Ray Observatory (CGRO) for gamma rays. SIRTF was launched in August 2003, and was commissioned in December 2003 as the Spitzer Space Telescope. For convenience, the names SIRTF and Spitzer Space Telescope will be used interchangeably in this paper. SIRTF has unprecedented sensitivity in the infrared, leveraging a large defense-based investment in the infrared detector arrays, with additional development under NASA sponsorship [18]. SIRTF will study the early universe, evolution of galaxies, birth of planetary systems, search for brown dwarfs, etc.

The orbit of SIRTF is unusual for a space telescope in the sense that it does not orbit the Earth. Rather, SIRTF orbits the Sun at 1 AU in an Earth-trailing orbit, which drifts away from Earth at about .12 AU per year (cf., Figure 1). This Heliocentric orbit is ideal for infrared science since it avoids the effect of the

¹ Senior Research Scientist, Jet Propulsion Laboratory, California Institute of Technology, 4800 Oak Grove Drive, Pasadena, CA, 91109, E-mail: david.bayard@jpl.nasa.gov. Phone: (818) 354-8208, FAX: (818) 393-4440.

Earth/Moon system as a huge heat disturbance source. To support the sensitivities required for infrared astronomy, SIRTf is cryogenically cooled down to below 5.5 degrees Kelvin. The consumption of cryogen fundamentally limits the life span of SIRTf, and drives the need for high operational efficiency. The nominal expected mission life is 2½ years, with a goal of 5 years. The SIRTf mission is managed for NASA by the Jet Propulsion Laboratory. The main engineering contractors are Lockheed Martin (for the spacecraft bus and integration) and Ball Aerospace (for the telescope optics and cryogenic assembly). A general description of the observatory is given in reference [1].

This paper discusses the pointing control system for SIRTf, providing an overview of the pointing control hardware, pointing architecture, pointing requirements and capability, attitude constraints/commanding, required calibrations, and attitude observers.

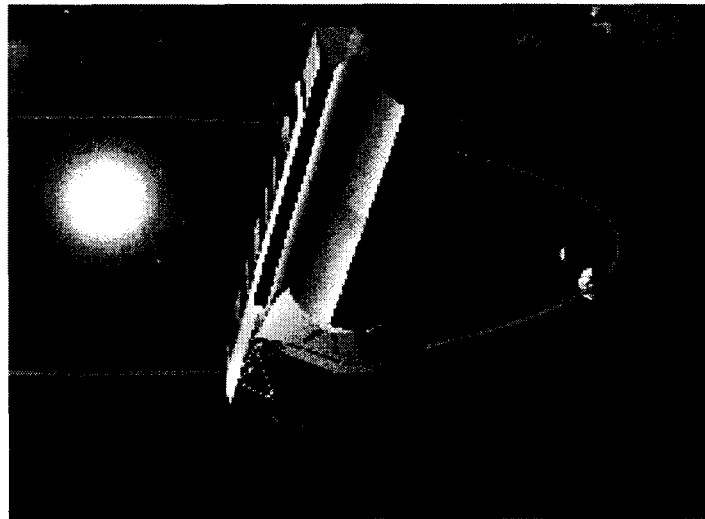


Figure 1: Artist's rendering of SIRTf in its Heliocentric, Earth-trailing orbit.

OVERVIEW OF TELESCOPE

The telescope optics are shown in Figure 2. The primary mirror is 85 cm, and is of a Ritchey Chretien design which ensures that the optics are well compensated for spherical aberration and coma. The optics are diffraction limited to 6.5 μm , and are designed to operate at or below 5.5 degrees Kelvin. The focal length is 10.2 meters with a focal ratio of $f/12$. The field of view is 32 arcmin (approximately the size of the full moon as seen on the sky), with a spectral bandpass between 3 and 180 μm .

The focal plane layout is shown in Figure 3. This particular figure looks down into the telescope and will look different when projected on the sky (cf., Figure 6). It is seen that SIRTf carries three scientific instruments: the Infra-Red Array Camera (IRAC) which provides images from 1.8 to 27 μm ; the Infra-Red Spectrograph (IRS) which provides spectra from 4 to 200 μm ; and the Multiband Imaging Photometer for SIRTf (MIPS) which provides images and large area mapping from 20 to 200 μm . MIPS is unique in that it uses a scanning mirror to extend its field of view, and to coordinate with synchronized spacecraft scanning motions.

Also included in the focal plane are two Pointing Control Reference Sensors (PCRSs). The PCRS is a 4x4 pixel array, with 10 arcsecond pixels. Interestingly, the PCRS is the only real estate in the focal plane which is owned by the pointing control system. This restriction is intentional since the heat dissipation from a more significant pointing sensor in the cooled focal plane (e.g., such as HST's fine guidance sensor) would be prohibitive and significantly shorten the life of the mission.

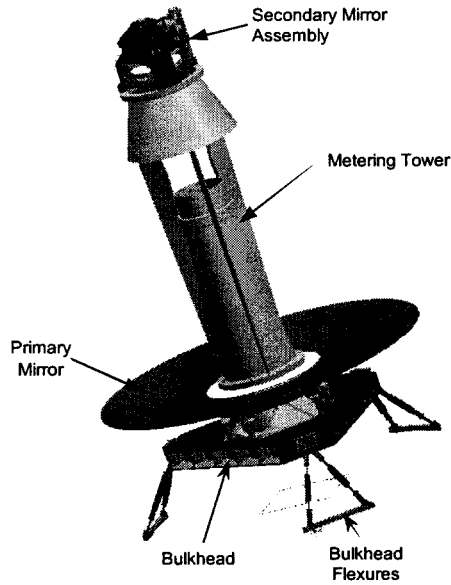


Figure 2: SIRTTF telescope optics

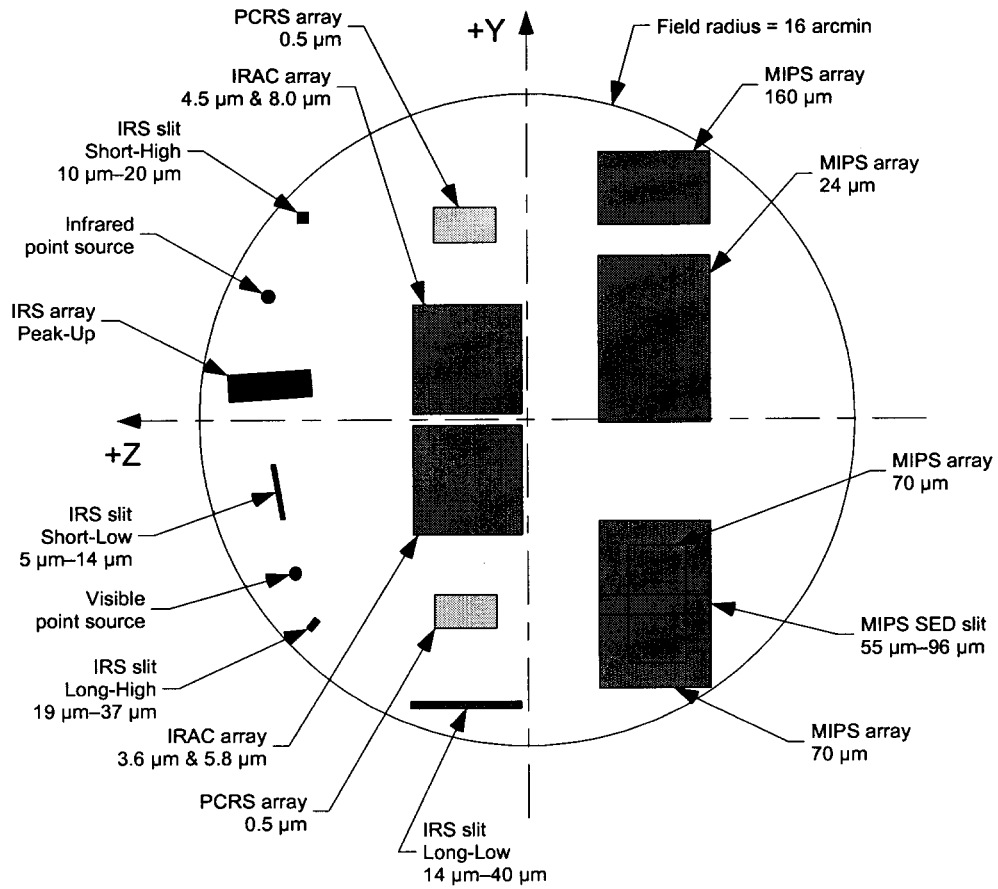


Figure 3: Focal plane layout (looking down into the telescope)

POINTING CONTROL HARDWARE

The SIRTf spacecraft is shown in Figure 4. The Pointing Control System (PCS) is a celestial-inertial, three-axis stabilized control system. The SIRTf pointing control hardware includes: 2 Kearfott SKIRU V gyro boxes (4 gyros per box), 2 LMMS AST 301 star trackers, 4 Ithaco B reaction wheels (all used simultaneously), 2 fine and 3 coarse LMMS sun sensors (the fine sensors are actually finely calibrated versions of the coarse sensors), and 2 specially designed Pointing Calibration Reference Sensors (PCRS) to provide a pointing reference that lies within the telescope focal plane. A cold gas Reaction Control System (RCS) is available which makes use of cold-gas thrusters for momentum dumping, but is not used for pointing purposes.

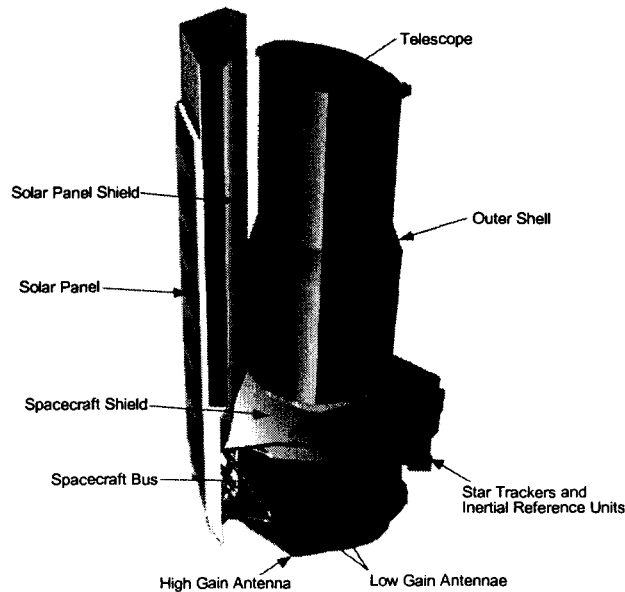


Figure 4: Spacecraft configuration

The LMMS AST 301 star tracker (cf., Figure 5) is modified from an earlier AST 201 model to provide higher accuracy [17]. The main modifications are a reduced FOV, redesigned optics, larger star catalog, and an upgraded processor. The star tracker has a 5x5 degree FOV, tracks up to 50 stars (20 at the galactic poles, 40 typically), and provides updates at a rate of 2 Hz. At the Galactic equator, the tracker must provide an overall NEA of 0.20" (x,y), 5.5" (z), and a bias of 0.57" (x,y), 19" (z). At the Galactic poles where the stars are more sparse, the tracker has a slightly less stringent requirement to provide an overall NEA of 0.22" (x,y), 6.2" (z), and a bias of 0.62" (x,y), 21" (z).

Only one star tracker is used at any one time, and both are nominally boresighted in the same direction as the telescope boresight. The AST 301 is completely autonomous (requires no initialization) and outputs a full quaternion measurement of attitude. Autonomous identification of stars is carried out using an on-board catalog of 87,000 Tycho stars down to 9th visual magnitude. The Star Tracker requirements (for Galactic equator) along with a preliminary assessment of in-flight performance is summarized in Table 1. It is seen that the delivered AST 301 tracker performs better than the requirement by a factor of two in NEA and by a factor of at least three in bias. In practical terms, this improved star tracker performance has trickled down to provide increased margin, and improved pointing performance across all aspects of the SIRTf pointing control system.

The SKIRU V gyros have been used previously on Chandra and various LMMS missions. They have an angle random walk of 56e-6 deg/rt-hr, a bias stability of 0.0045 deg/hr, and they have been designed

specially for SIRTf to have a small angle quantization of 0.005 arcsec. At a sampling rate of 10 Hz this gives an effective rate quantization of 0.05 arcsec/sec (suitable for solar system object tracking).

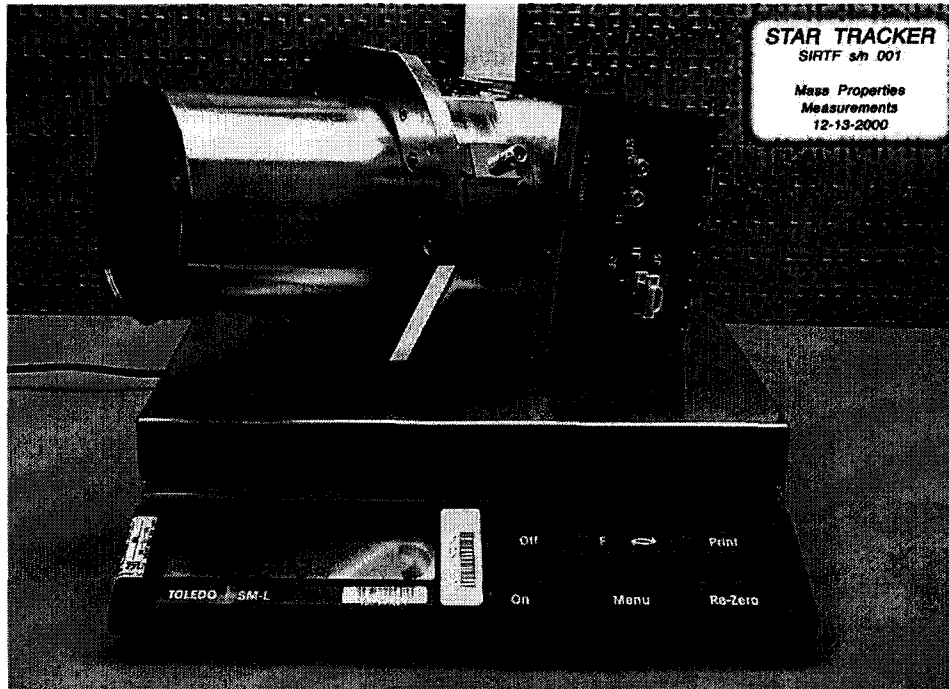


Figure 5: LMMS AST 301 Star Tracker (courtesy of Roel Van Bezooijen, Lockheed Martin)

Table 1.
STA requirements and in-flight performance (arcsec, per-axis, 1-sigma, at Galactic equator)

	NEA (per-axis / Twist)	BIAS (per-axis / Twist)
Requirement	0.20 / 5.5	0.57 / 19
In-Flight (approx)	0.11 / 2.5	0.2 / 5.3

The Ithaco Type B reaction wheels are commandable to a max torque of 0.04 Nm with a 8 bit quantization, and have a 19 Nms storage capability. The static imbalance is $2.16e-5$ Kg-m, the dynamic imbalance is $3.6e-6$ Kg-m², the torque ripple is 10% and the cogging torque is 0.002 Nm. All four reaction wheels are used simultaneously for pointing purposes, taking advantage of the null-space for momentum management.

Two Pointing Calibration Reference Sensors (PCRS) lie in the telescope focal plane, and provide a alignment reference for telescope pointing [16]. Each PCRS sensor has an A and B side, of which only the A side is active - the B side is used only if the A side fails. Each pixel of the PCRS is 250 microns square, with a plate scale of 10 arcsec per pixel. The PCRS is sensitive down to 10th visual magnitude, with a center wavelength of 0.55 um. The central four pixels are extremely well calibrated for pointing alignment purposes, providing 0.14 arcsec centroiding accuracy, 1-sigma, radial.

POINTING REQUIREMENTS AND IN-FLIGHT PERFORMANCE

The pointing requirements are outlined in Table 2, along with a preliminary assessment of the in-flight performance, and a comparison with pre-flight predicted capability [12][2].

Table 2.
Pointing requirements and capability (arcsec, 1-sigma, radial)

Pointing Requirements and Capability			
	Reqmt	In-flight Performance ¹	Pre-flight est (cf., [2])
Pointing accuracy	5"	0.45" (ref [5])	2.34"
Incremental offset accuracy	0.56"	0.55"	0.37"
Stability over 200 sec	0.3"	0.02" (cf., [21])	0.06"
Stability over 500 sec	0.6"	0.02" (cf., [21])	0.11"
*Scan stability over 15 sec	0.7"	0.23"	0.23"
*Scan stability over 150 sec	1.0"	0.24"	0.24"

* assumed to be at scan rates from 2 to 20 arcsec/sec
¹Preliminary assessment

KEY POINTING FRAMES

The main Instrument Pointing Frames (IPFs) of interest for pointing are shown in Figure 6. IPFs are defined by specific pixel locations in each science array, which adopt the orientation of the pixel rows and columns. The quaternions for 128 such IPFs are stored in an on-board database, denoted as the "Frame Table". A typical pointing command specifies that a particular frame from the Frame Table (denoted by its number) should be pointed to a particular location on the sky (denoted by its RA and DEC). The attitude commander applies a velocity aberration correction to the RA,DEC position and then computes an attitude which points the desired frame to the desired location on the sky, subject to the geometric attitude constraints. Details on the attitude constraints are discussed next.

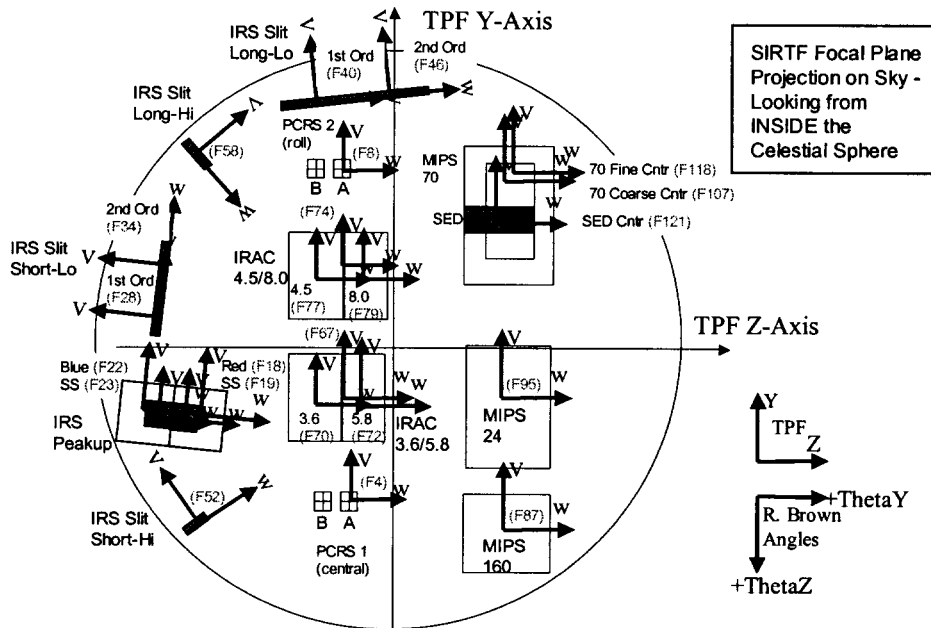


Figure 6: Key instrument pointing frame

ATTITUDE CONSTRAINTS

The attitude constraints for SIRTf are shown in Figure 7. The telescope is restricted to pitch at most -10 degrees toward the sun (sun avoidance on the CTA) and 30 degrees away from the sun (power constraint). The roll angle is constrained to +/- 2 degrees (not shown). The yaw angle is unconstrained.

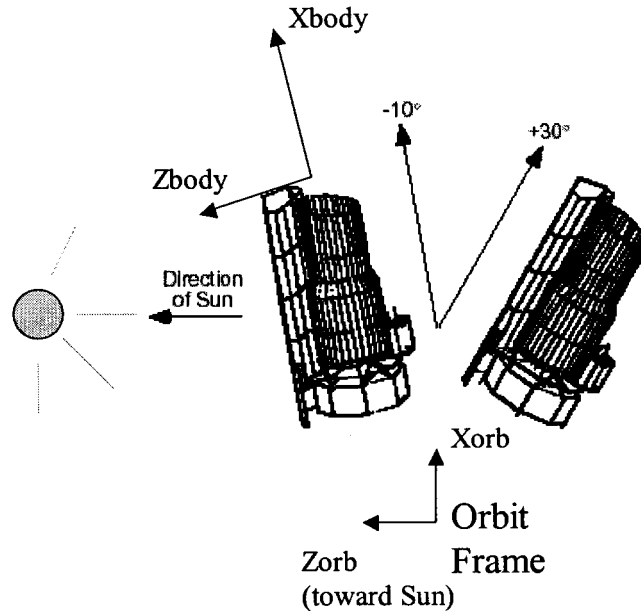


Figure 7: SIRTf attitude pitch angle constraint

Mathematically, one can write these constraints concisely as follows. The constraint is written with respect to the cryogenic-telescope assembly (CTA) frame, which is defined by the sun-shield geometry (but is nominally aligned with the telescope boresight frame). Let the orbit-to-CTA frame transformation be denoted by D_{orb}^{cta} , and be decomposed into its Euler 3,2,1 sequence as follows,

$$D_{orb}^{cta} = R_1(\theta_1)R_2(\theta_2)R_3(\theta_3)$$

Then the attitude constraints at any time instant can be written as,

$$-10^\circ \leq \theta_2 \leq 30^\circ$$

$$-2^\circ \leq \theta_1 \leq 2^\circ$$

Note, that the yaw angle θ_3 remains unconstrained.

Fixed Attitude Commanding

The attitude commander must take into account the constraints discussed above. In its simplest case of commanding a fixed reference attitude, the ground specifies,

- (i) A Frame Table number (desired frame to point)
- (ii) An RA,DEC (the desired sky location, corrected on-board for velocity aberration)
- (iii) A value for θ_1 , denoted as the roll constraint angle (RCA)

The attitude commander fixes the value $\theta_1 = RCA$ in the expression above for D_{orb}^{cta} , and then solves for the θ_3, θ_2 angles that point the boresight of the frame specified in (i) to the sky location in (ii). Typically the RCA angle is specified as 0, unless one is holding the same attitude for many hours, in which case the orbital rotation must be taken into account.

Point-to-Point Attitude Commanding

The attitude commanding is briefly discussed in this section. Full details can be found in [4].

The attitude constraint region is shown in Figure 8. Often SIRTf starts at a fixed attitude within the constraint region, and desires to maneuver to another attitude within the constraint region (computed using the procedure from the previous section). The procedure for the designing the attitude path is simply to connect the start and end points in Figure 8 with a straight line. This entire path is guaranteed to lie within the constraint because the end-points do, and the constraint region is convex. The reaction wheel torques are shaped to accelerate, coast and decelerate along this straight-line path. Note that this path in general does not correspond to a simple single axis (i.e., eigen-axis) rotation.

POINTING CONSTRAINT REGION

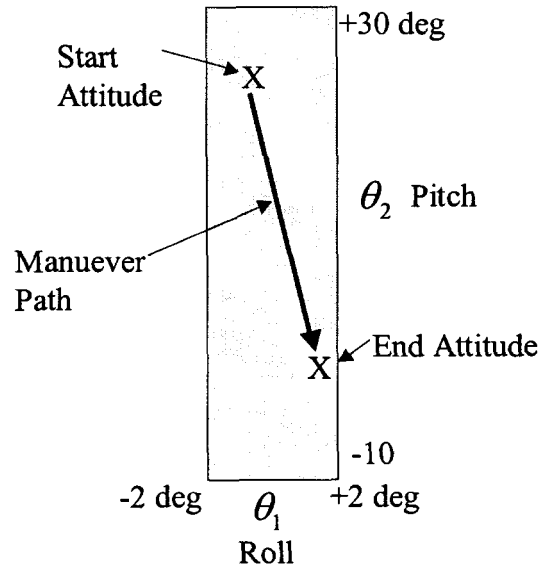


Figure 8: Attitude maneuvers using straight line segments in Euler angle space

POINTING FRAMES AND TRANSFORMATIONS

The key pointing frames and frame transformations for SIRTf are shown in Figure 9. They will be in more in more detail in this section.

The International Celestial Reference System (ICRS) frame serves as SIRTf's principle inertial reference frame. With a suitable relabeling, the star-tracker instrument frame serves as the SIRTf Body frame (i.e., when spelled with its boresight as the x axis – see [10]). The mapping from ICRS to the Body Frame is denoted as the spacecraft attitude A .

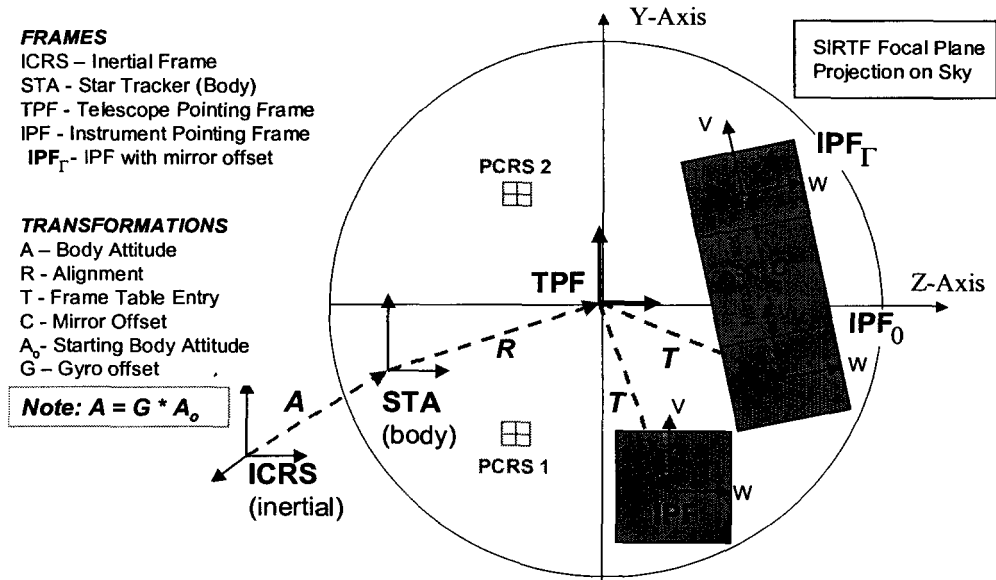


Figure 9: Main SIRTf Pointing Frames and Transformations

The Telescope Pointing Frame (TPF) has the telescope boresight as its x axis, and is defined rigorously in terms of the null points of the two PCRS sensors in [10]. The mapping from the Body Frame to the TPF is denoted as the alignment matrix R.

As mentioned earlier, Instrument Pointing Frames (IPF) are defined by specific pixel locations in each science array and which adopt the orientation of the pixel rows and columns. The mapping from the TPF to any specified IPF is denoted as T. The IPF frames are stored in an on-board “Frame Table” as 128 values for T (stored as quaternions). Certain important IPF frames are denoted as **Prime Frames** (e.g., typically located at the center of each of the instrument arrays). Other frames are called **Inferred Frames** and are defined by a pixel offset relative to a nearby Prime frame. The nominal orientations of the science instruments and their associated Prime frames in the telescope focal plane have been shown earlier in Figure 6. Also seen are the associated w and v directions associated with each frame, which are used by the attitude commander for implementing fixed angle pointing offsets.

The C matrix represents a scan mirror offset from a nominal starting position $\Gamma = 0$ to its current local mirror position $\Gamma \neq 0$ (where Γ is the commanded scan mirror rotation angle, in radians). For non-MIPS instruments, the C matrix is set to identity. For MIPS, the frame defined when the mirror is at position Γ is denoted as IPF_{Γ} . Note that as the scan mirror moves there is an entire family of IPF_{Γ} frames generated as a continuous function of the variable Γ .

The C matrix is not used for pointing purposes, although it is used for pointing reconstruction. Because of this the key frames for pointing are A, R, and T which can be remembered because they spell the common word “art”. These important frames will be discussed in more detail in the architecture section. The attitude A is time-varying due to telescope repositioning, and R is time-varying due to thermo-mechanically induced alignment drift. The mapping T is assumed constant due to the fact that the telescope focal plane is actively cooled. The mapping C is time-varying due to a time-varying, and nominally known, scan-mirror offset angle Γ .

POINTING CONTROL SYSTEM

A schematic of the pointing control system architecture is shown in Figure 10. Here, the quaternions q_A, q_R and q_T , represent the transformations A,R and T, defined earlier. The sensor signals shown on the left are mapped through the diagram to create a control error shown on the right. The controller acts to null the indicated error. The main estimation filters used by the pointing control system are listed in Table 3.

The gyro rate (actually an incremental angle) is sampled at 10 Hz and is first corrected for scale factor and alignment, and then for bias by the Gyro Calibration Filter (GCF). The compensated rate and star tracker quaternion (available at 2 Hz) are then input into the attitude observer. One of three time constants for the attitude observer can be chosen by use of gain switching. In addition, the attitude can be propagated purely by integrating the gyro rate estimate. This requires logic to provide an initial starting attitude estimate from the attitude observer, after which the rate estimate is integrated numerically. Selection logic chooses whether the attitude observer or gyro-propagated quaternion estimate is used for control purposes.

If one is commanding SIRTf over a long periods based on gyro-only propagation (i.e., tens of minutes) an "attitude reset" command can be issued which resets the gyro integrator with the observer attitude quaternion at the time of the command, and continues propagating from this attitude. This causes a momentary discontinuity in the controlled attitude position, but acts to remove any accumulated attitude error which built up over time due to the gyro drift.

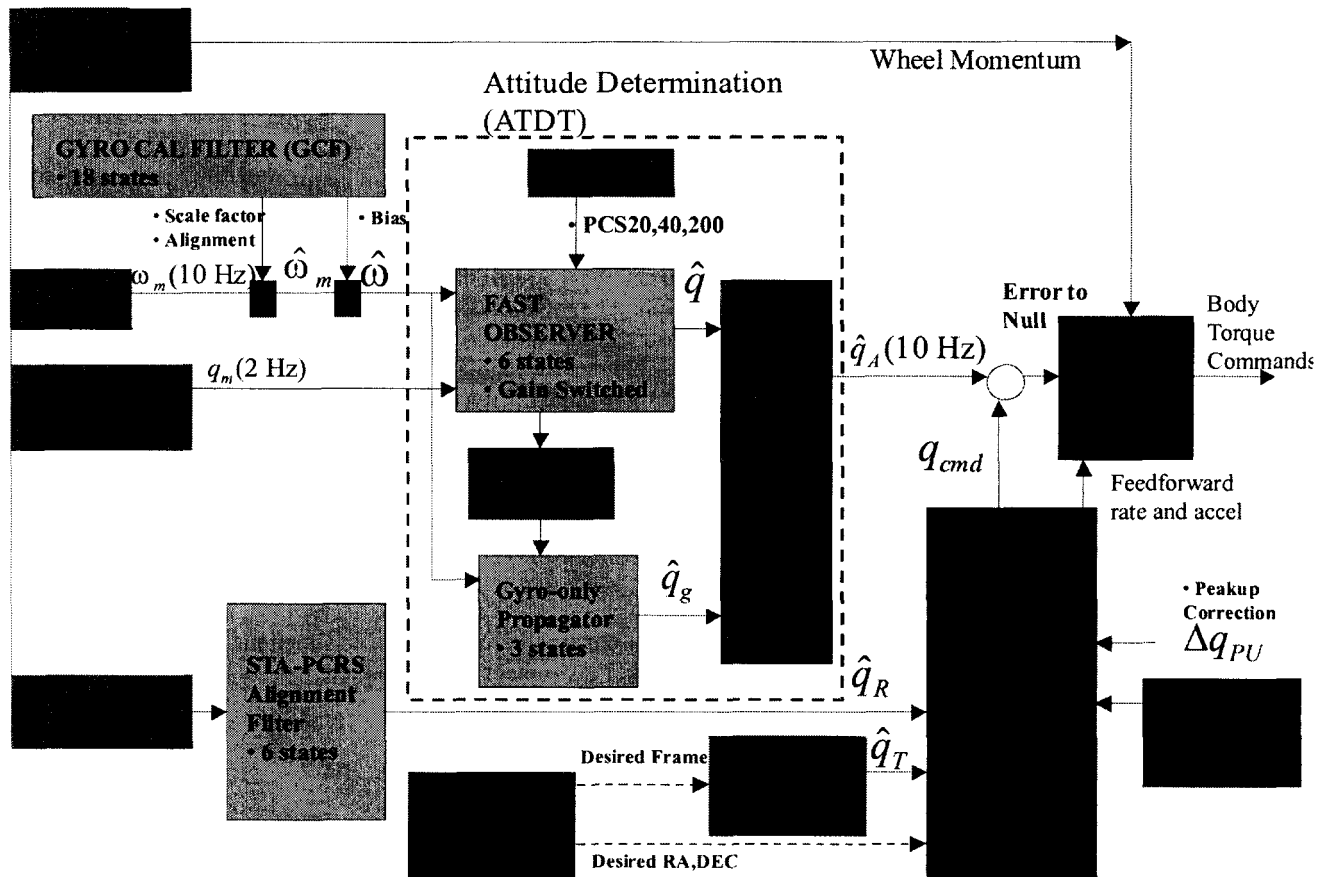


Figure 10: SIRTf Pointing Control System Architecture Schematic

The frame alignment R is recursively estimated on-board by the STA-PCRS alignment filter (sometimes denoted as the S2P filter). The STA-PCRS alignment filter is a six state Kalman filter which was developed at JPL, and flight implemented by Lockheed Martin [9]. Its main input is a PCRS centroid and an attitude estimate, and its main output is a recursive estimate of R . A centroid is taken on a single PCRS once every 8 hours to feed this filter and maintain the accuracy of R to $\frac{1}{2}$ arcsecond (y,z directions). Even though a single star is used at each update, the filter is able to estimate the twist alignment because successive updates alternate between using PCRS1 and PCRS2. The twist angle knowledge of R is maintained in this fashion to within 10 arcseconds error. A similar pointing filter on the ground, denoted as the Pointing Alignment and Calibration (PAC) filter is used during IOC which repeats the calculations of the STA-PCRS alignment filter, but estimates an additional parameter related to the separation distance between the two PCRS sensors.

The Frame Table contains 128 quaternion values for the various TPF-to-IPF mappings T , needed for pointing. The attitude commander takes a specified Frame Table quaternion and desired RA,DEC location and then computes the desired pointing attitude. The SIRTf ephemeris is also provided to the attitude commander to compute the orbit frame (needed for constraint avoidance) and to compute a velocity aberration correction which is applied to the desired RA, DEC pointing direction.

Like the Hubble Space Telescope, SIRTf uses an attitude observer rather than a Kalman filter to avoid the long settling times associated using the optimal smoothing filter. Interestingly, although the Kalman filter is optimal, it has a very sluggish pole (i.e., a real pole near the origin) which significantly lengthens settling times and makes it less desirable for use when efficiency is an issue. Instead, SIRTf uses 3 Fast Observers which are designed by solving an optimization problem which minimizes the variance of the attitude estimate subject to a constraint that the poles of the filter lie to the left of a line in the left-hand Laplace s -plane. Fast Observers will be discussed in more detail later.

The GCF is an on-board Kalman filter with 18 states which was developed at JPL, and flight implemented by Lockheed Martin [11]. The GCF filter includes 9 linear scale factors and alignments, 3 attitude states, 3 bias states, and 3 absolute scale factor parameters. The GCF scale factor and alignment parameters are calibrated using $1\frac{1}{2}$ hours of dedicated maneuvers every fourth day (i.e., $\frac{1}{2}$ hour per axis). This maintains calibration to approximately 95 parts per million. The GCF bias parameters are updated based on inertial hold data. Regular inertial holds are built into the commanded sequences such that there is a 100 second inertial hold at least every 3 hours (or every 15 minutes for high accuracy .0008 arcsec/sec bias cal). Since the attitude observer has six states (3 attitude, 3 gyro bias), it includes an extra level of compensation for the gyro bias. However, this extra level of compensation is only available during observer-based pointing and not for gyro-only attitude propagation.

The Frame Table entries are estimated using a ground-based Instrument Pointing Frame (IPF) filter. The IPF filter is a 37 state Kalman filter that was developed at JPL [10][14]. The IPF filter is ground-operated at JPL, and determines all essential IPF frames, plate scales and optical distortions.

There are various other calibration filters that not covered here, for specific functions such as sun-sensor calibration, PCRS instrument calibration, star tracker instrument calibration, etc.

Table 3.
Main estimation filters used by the SIRTf pointing control system

FILTER	# states	Description	OPS	Update Frequency
Fast Observer	6	Attitude Observer 3 – attitude states 3 – gyro bias states Switched gains for 20,40, 200 second time constants	Flight	Continuous (2 Hz tracker, 10 Hz gyro)
STA-to-PCRS (S2P)	6	Tracker to telescope alignment 3 –short-term alignment drift 3 – long-term alignment	Flight	Every 8 hours
GCF	18	Gyro Calibration Filter 3 - scale factors 6 - misalignments 3 – absolute scale factors 3 – gyro bias 3 – attitude	Flight	- Calibrate scale factors & alignment for 1.5 hours every fourth day - Calibrate gyro bias every (>100sec) inertial hold opportunity
PRI	11	Pointing Ready Indicator - signals earliest time after slew suitable to take observation 4 –2 states per 2-axis rigid body 7 – controller states	Flight	Every slew that is controlled based on the attitude observer
IPF	37	Instrument Pointing Frame Filter - Focal Plane Calibration: 37 - Pointing alignments, plate scale parameters, optical distortions	Ground	Several times for each Prime Frame during in-orbit checkout period
PAC	7	Pointing Alignment and Calibration filter 6 – same as STA-to-PCRS 1 – angle between the two PCRS	Ground	Multiple times during in-orbit checkout period

FAST OBSERVERS

As mentioned earlier, SIRTf does not use a Kalman filter for attitude determination. The reason for this is that a sluggish pole from the optimal Kalman filter significantly slows settling time. The solution is to design attitude observers that settle fast but still have good (but not necessarily optimal) smoothing properties. Such attitude observers are denoted as Fast Observers, and their theory is treated in [8]. Fast Observer design is briefly outlined here, as applied to the SIRTf pointing control system.

In terms of the Laplace s variable, a two-gain decoupled attitude observer that combines measurements from a gyro and star tracker can be written as follows,

Attitude Observer (Decoupled)

$$\hat{\theta} = \frac{(sk_1 + k_2)y + s^2(\omega_m / s)}{s^2 + k_1s + k_2}$$

$$\hat{b} = \frac{k_2(\omega_m - sy)}{s^2 + k_1s + k_2}$$

y - Angle meas (star tracker with NEA)

ω_m - Rate meas (Gyro, with bias and ARW)

θ - Angle (attitude)

b - Rate bias

Let the variance of the estimate $\hat{\theta}$ be written as a cost function $J(k_1, k_2)$ to be minimized,

$$J = \text{Cov}[\theta - \hat{\theta}] = J(k_1, k_2)$$

Then the optimal steady-state Kalman filter corresponds to the solution of the following minimization problem,

Steady-State Kalman Filter

$$\min J(k_1, k_2)$$

$$k_1, k_2$$

However, the Kalman filter solution does not place any constraint on the settling time, and the resulting filter can be quite sluggish. This is particularly true in fine pointing applications where the steady-state Kalman filter is often a split-root real pole design with one of the poles very close to the origin.

Consider instead the Fast Observer design which is defined by the solution to the following constrained minimization problem,

Fast Observer

$$\min J(k_1, k_2)$$

$$k_1, k_2$$

subject to

$$\text{Real (poles of } s^2 + k_1s + k_2) \leq -\frac{1}{\tau}$$

Here, the variance is minimized subject to a constraint that the poles be sufficiently fast. Specifically, the poles are constrained to be located to the left of a specified line in the Laplace plane, which ensures that the response will be on the order of τ seconds. A globally optimal analytic solution to the Fast Observer problem is given in [8], based on solving the corresponding Kuhn Tucker conditions.

Interestingly, for sufficiently fast Fast Observers, the solution is always a double pole located on the real axis at $-1/\tau$, so that $k_1 = 2/\tau$ and $k_2 = 1/\tau^2$. For slower Fast Observers, the design is more complicated but can still be calculated analytically.

The SIRTTF pointing control system uses 3 Fast Observer designs with the time constants $\tau = 20, 40, 200$, respectively. The values for these designs is given in Table 4 and Table 5. The k_1, k_2 gains from these designs are input into a free running second-order filter structure using gain-switching logic. The gains for the (x) axis (i.e., the noisy twist axis) observer are not switched, but are kept constant and consistent with a 200 second time constant for maximum smoothing.

Table 4
Fast Observer gains for (y,z) axes

Observer Gains for (y,z) axes		
τ	k_1	k_2
200	.031225	.00013113
40	.05	6.25e-4
20	.1	.0025

Table 5.
Fast observer gains the (x) axis

Observer Gains for (x) axes		
τ	k_1	k_2
200	.01	2.5e-5

INCREMENTAL OFFSET PROCESS

One of SIRTf's most difficult pointing challenges is to support IRS spectroscopy measurements by placing target sources into the center of very narrow slits. For example, the Short-Hi slit is only 4.7" wide and Short-Lo slit is only 3.6" wide, and it is desired to place the source to within 0.56" (1-sigma, radial) of the center of these slits.

Incremental Pointing Procedure

The overall procedure used to place an IR object into a spectroscopy slit is shown in Figure 11. Here, the source is first centroided on the IRS Peak-up array to get a coarse estimate of its location. The source is then moved and centroided on a more accurately calibrated portion of the Peak-up array (denoted as the Sweet-Spot) to get a fine estimate of its location. Then an offset maneuver is calculated in real-time to move the source from the Peak-up array to the slit center.

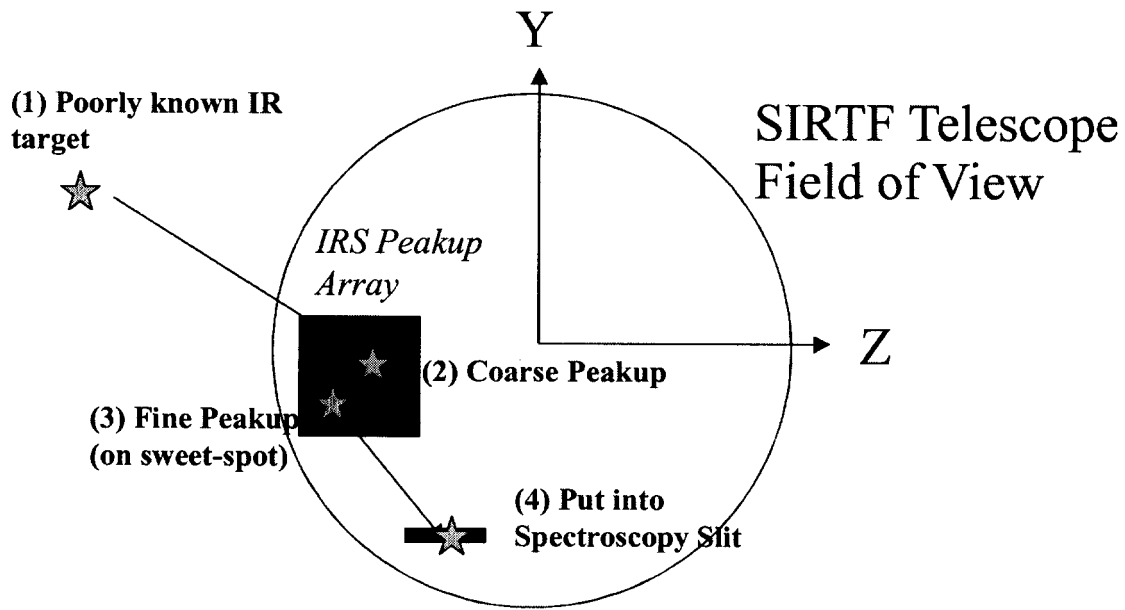


Figure 11. The peak-up and incremental offset procedure for putting sources onto spectroscopy slits

This offset procedure requires that the following issues are properly addressed,

- (i) an accurate real-time centroid measurement is taken on the Peakup array,
- (ii) the Peakup array position is accurately known relative to the slit position in the focal plane.
- (iii) the incremental offset maneuver is executed accurately
- (iv) In long exposures, the gyro drift does not cause the target source to drift out of the slit

Issue (i) requires that the plate scales and optical distortions across the Peakup array have been accurately characterized in the focal plane survey, and that they are applied in-flight to correct the centroided position. Issue (ii) requires that the focal plane survey has also accurately characterized the relative frame locations in the focal plane. Issue (iii) requires that the gyro is calibrated accurately (scale factor, misalignment, and drift) to minimize propagation errors over short distances. These issues were addressed in the design stage by generating requirements on the respective component pointing errors, and calibration processes.

Issue (iv) arises because many of the spectroscopy exposures are of sufficient duration (500-3000 seconds) that the gyro drift can move the target source off the slit center and violate the spectroscopy requirements. Switching to the observer at this time will not solve the problem because the relative star tracker error incurred over the maneuver (from the Peakup array to the slit position) will come into play, and potentially violate the overall 0.56" offset requirement. For this reason, the incremental offset maneuver is implemented using a special reconfigurable control approach [7]. The reconfigurable control approach brings the observer back into play in such a way as to minimize the impact of the relative star tracker error incurred over the maneuver.

Reconfigurable Control

The reconfigurable control approach to incremental pointing is depicted in Figure 12. Here OBS1 and OBS2 are attitude observers having time constants τ_1 and τ_2 , respectively. OBS1 and OBS2 are both driven by the measurement position quaternion q_m and measured 3-axis rate ω_m . The observer OBSg generates an attitude estimate based on integrating the gyro rate from some specified initial quaternion. In this scheme, OBS1 and OBS2 are free running filters while the gyro propagation filter OBSg is initialized by OBS1 at $t=0$. In actual implementation, OBS1 and OBS2 are the same attitude observer. The errors e_1, e_2, e_g denote the attitude errors generated between each observer (OBS1, OBS1, and OBSg, respectively) and the commanded quaternion. Simply stated, e_1, e_2, e_g are the errors that are nulled by the attitude controller, depending on which observer is active at the time.

In the reconfigurable control approach, the attitude is controlled using the OBS1 attitude estimate, while the Peak-up centroid is being taken. Control is then switched to using the gyro-propagated OBSg quaternion for maneuvering the source over to the desired slit. Intuitively, after arriving at the slit, one would like to get off of gyros as soon as possible to avoid drifting out of the slit. Unfortunately, the OBS2 attitude estimate will generally not be settled immediately, so one is forced to wait. After a specified time at the slit, denoted as the "hand-off" time, the control is finally switched to using the attitude observer OBS2.

There are two main ideas behind the reconfigurable control. The first is to switch the commanded attitude reference to become the OBS2 attitude estimate exactly at the hand-off time instant (see the "One Shot" hold button in Figure 12). This procedure leaves the observatory near the gyro propagated attitude at the hand-off time, without creating a jump discontinuity associated with the hand-off process. The second idea is to optimize the hand-off time. Intuitively, an optimal hand-off time always exists because the observer settling error decreases with the time before hand-off, while the error from gyro drift increases during this same time period. The existence of an optimal hand-off time, and its optimization is discussed in [7]. The current hand-off time is set to 80 seconds, as determined by pre-flight simulations. However, in-flight performance indicates that there may be some benefit to decreasing the hand-off time somewhat, e.g., to 60 seconds or less. The optimization of the hand-off time along these lines is currently under study.

A preliminary assessment of in-flight performance indicates that incremental pointing is accurate to approximately 0.55" (1-sigma, radial), meeting the 0.56" requirement.

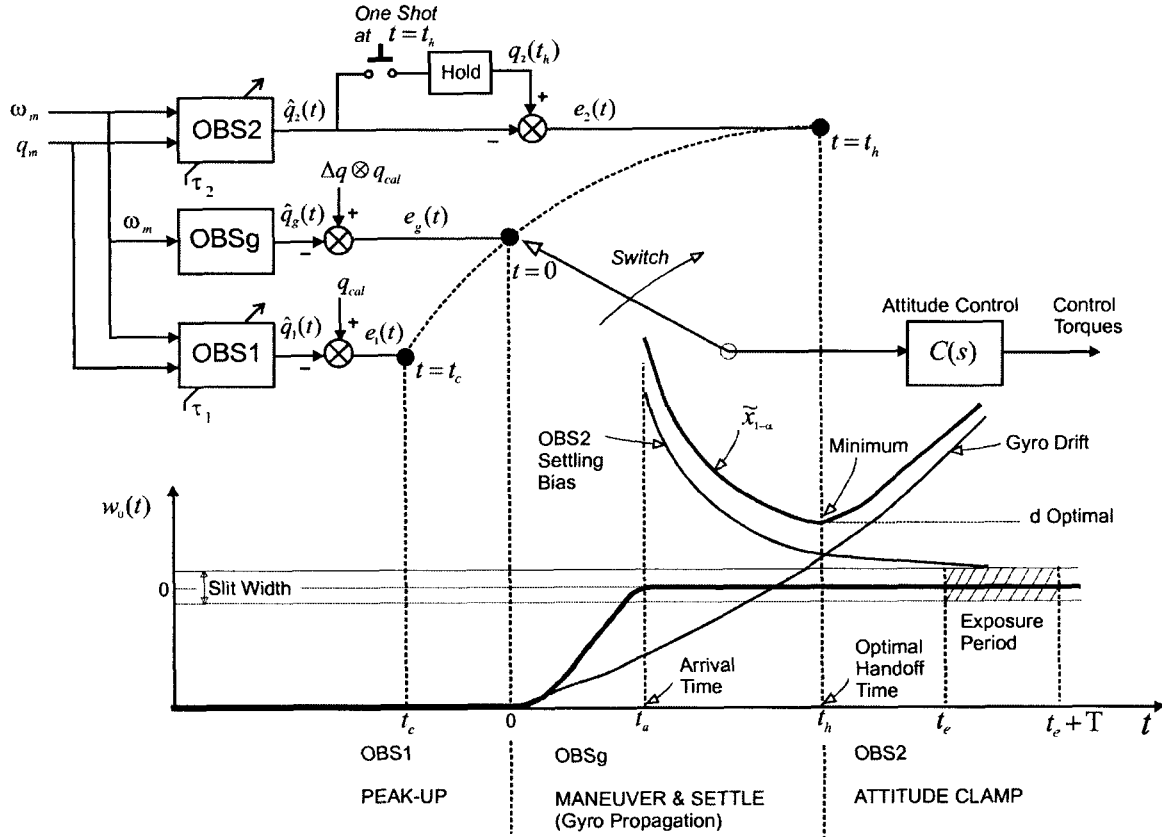


Figure 12. Reconfigurable control for incremental offset pointing

FOCAL PLANE CALIBRATION

Focal plane calibration is required to learn the position of each of the science arrays in the focal plane (i.e., the alignment matrices T depicted in Figure 9), as well as plate scales (i.e., the angular size of one's pixels) and optical distortion parameters. Prior knowledge about the focal plane is available from optical performance tests performed on the ground in the Brutus chamber at Ball Aerospace [19][20]. However, limitations in mimicking in-flight conditions and shifts due to launch loads require that the focal plane be recalibrated in-flight.

Because SIRTf's focal plane is actively cooled, it is only necessary to learn these calibration parameters once. After accurately learned and recorded during the in-orbit checkout period, these parameters are not expected to change over the course of the mission.

The calibration of the focal plane is performed using a series of experiments denoted as "sandwich" maneuvers. A generic sandwich maneuver is shown in Figure 13 and consists of the following sequence of steps.

1. Locate a target star on the first PCRS detector, PCRS 1, and take one or more centroid measurements.
2. Move the target star to PCRS 2, and take one or more centroid measurements

3. Move the target star to several positions on the desired science instrument array, and take a centroid measurement at each location (for example, a 3x3 grid pattern)
4. Return to the PCRS 1 detector, and take one or more centroid measurements.

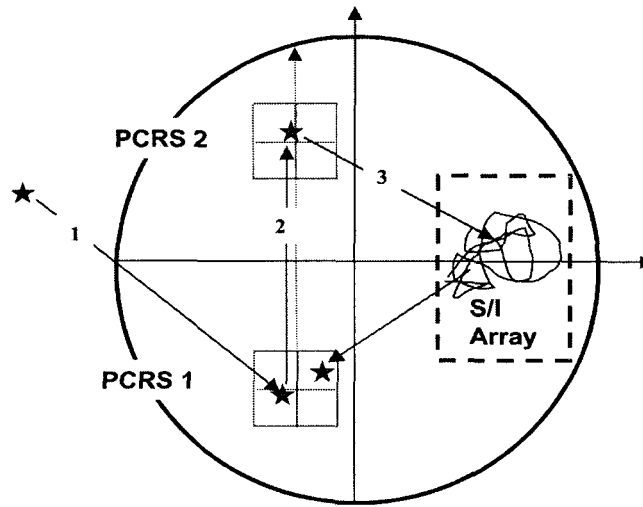


Figure 13. Generic sandwich maneuver format for focal plane calibration

The centroids taken on the science array are arbitrary, but must result in a time-tagged list of centroids (with both x and y coordinates). This approach is very general, allowing for grid patterns, dither patterns, simultaneous star clusters, etc. For the MIPS instrument, the time-tagged list of centroids includes additional information about the commanded scan mirror offsets, so that the scan mirror can be calibrated with respect to scale factor and alignment (i.e., along track and cross-track type errors). For IRS spectroscopy slits, the centroids are “faked” in the sense that the source is scanned across the slit and the centroid is reported at the center of the slit at the time instant of maximum flux.

The Telescope pointing frame (TPF) is defined in terms of the location of the two PCRS boresight unit vectors (i.e., reference frame defined by measurements). By transitioning between the two PCRS and the science array, the sandwich maneuver is informative about the location of the IPF with respect to the TPF (i.e., the alignment matrix T in Figure 9), and the TPF with respect to the body frame (i.e., the alignment matrix R in Figure 9). Also, by beginning and ending on the same PCRS, the sandwich maneuver is informative about accumulated attitude error due to gyro drift, which can be calibrated out accordingly. The sandwich maneuvers are repeated a statistical number of times to ensure that the random errors can be adequately reduced by smoothing the data.

A 37 state Instrument Pointing Frame (IPF) Kalman filter was designed to process the sandwich maneuver data. The IPF filter is described in more detail in [10][14]. The IPF filter is novel in the sense that it combines engineering parameters (e.g., pointing errors, misalignments, gyro bias) and science parameters (e.g., plate scales, optical distortions), into the same filter formulation. This makes the calibration process very efficient and accurate, compared to many missions which estimate these parameters separately. One product of the IPF filter is an accurate estimate of the IPF frame (the frames T in Figure 9), which is used for updating the on-board Frame Table for supporting precision pointing. The calibration accuracies that have been obtained from running the IPF filter have been reported in [15] and are summarized in Table 6 (Prime frames only). The accuracies are compared to the requirements as specified in [4], and the pre-flight predictions of what accuracies were to be expected. It is seen that the calibration requirements are all met, and are close to their pre-flight predictions.

The MIPS calibration accuracies should be taken as preliminary, due to certain difficulties that were encountered while calibrating the various arrays (stray light, non-repeatability in the scan mirror, loss of half the 70 μm array, etc.) It is expected that the MIPS frames will be recalibrated at a later time.

Table 6.
Instrument Pointing Frame Calibration Accuracies (Prime Frames only)

Frame	Run	Description	CALIBRATION ACCURACY		
			Predicted	Actual	Requirement
			(arcsec) 1-sigma, radial		
018	501	IRS Red PeakUp FOV Center	0.1279	0.0899	0.25
019	502	IRS Red PeakUp FOV Sweet Spot	0.1009	0.0866	0.14
022	503	IRS Blue PeakUp FOV Center	0.1285	0.0968	0.25
023	502	IRS Blue PeakUp FOV Sweet Spot	0.1014	0.0868	0.14
028	502	IRS ShortLo 1 st Ord Center Pos	0.1056	0.1165	0.14
034	502	IRS ShortLo 2 nd Ord Center Pos	0.1061	0.0909	0.14
040	502	IRS LongLo 1 st Ord Center Pos	0.2571	0.1295	0.28
046	501	IRS LongLo 2 nd Ord Center Pos	0.2587	0.2682	0.28
052	502	IRS ShortHi Center Position	0.1037	0.0885	0.14
058	501	IRS LongHi Center Position	0.1864	0.1027	0.28
068	502	IRAC Center of 3.6umArray	0.1358	0.0881	0.14
069	502	IRAC Center of 5.8umArray	0.1359	0.0889	0.14
075	502	IRAC Center of 4.5umArray	0.1103	0.0878	0.14
076	502	IRAC Center of 8.0umArray	0.1103	0.0895	0.14
087	504	MIPS 160um Center Large FOV	0.2413	0.3694	3.70
095	602	MIPS 24um Center*	0.1235	0.0884*	0.14
107	201	MIPS 70um Center*	0.2957	0.4898*	2.60
118	203	MIPS 70um Fine Center*	0.2117	0.3013*	1.10
121	504	MIPS SED Center*	0.6392	0.3988*	1.10

* Preliminary

OTHER POINTING ISSUES

There are many interesting issues related to the SIRTf pointing system which have not been covered here. These areas include fault protection, pointing criteria for high-resolution spectroscopy [6], pointing reconstruction [13], among others. The reader is referred to the literature for further details.

CONCLUSIONS

SIRTf is NASA's new space telescope which is has been commissioned as the Spitzer Space Telescope. The on-board infra-red science instruments include cameras, scanning arrays, peakup arrays, and spectrographs. An overview of SIRTf's pointing control system has been given in the paper to give the reader a sense of how it has been architected and designed in order to address a wide range of challenging pointing accuracy, jitter, scanning, incremental offset, and efficiency requirements. Novel aspects of the pointing control system design have been highlighted and a preliminary assessment of in-flight performance has been provided.

ACKNOWLEDGEMENTS

This work was performed at the Jet Propulsion Laboratory, California Institute of Technology, under contract with the National Aeronautics and Space Administration. The author would like to thank Fernando Tolivar, Tooraj Kia and Keyur Patel of JPL, and Bill Clark, Dan Swanson, Rick Dodder, Greg Andersen, and the whole PCS team at Lockheed Martin for many fruitful collaborations.

REFERENCES

- [1] N. Vadlamudi and J. Miles, Space Infrared Telescope Facility, *Observatory Description Document*, LMMS/P458569, 674-SEIT-300, Version 1.2, November 1, 2002
- [2] G. Andersen, "Observatory Level Pointing Requirements Verification," Internal Document, SIRTf EM OSE-188, Rev A, January 20, 2003.
- [3] T. Alt, "PCS Pointing Command Algorithms," Internal Document, SIRTfEM PCS-130, April 4, 2001.
- [4] J. Miles and J.H. Kwok, "The SIRTf In-Orbit Checkout and Science Verification Plan," IR Space Telescopes and Instruments. Edited by John C. Mather. Proceedings of the SPIE, Volume 4850. pp. 141-152, 2003; more details in: *SIRTf In-Orbit Checkout and Science Verification Mission Plan*, 674-FE-301 Version 1.4, Internal Document, JPL D-22622, February 8, 2002.
- [5] D. Swanson, "Verification of PICD Requirement 3.7.1.1 – Absolute Pointing," Internal Document, SIRTf EM SESMO-04-0036, January 19, 2004.
- [6] D.S. Bayard, "Spacecraft Pointing Control Criteria for High Resolution Spectroscopy," IEEE Transactions on Aerospace and Electronic Systems, Vol. 35, No. 2, pp. 637-644, April 1999; more details in: D.S. Bayard, Internal Document, JPL D-14845, August 29, 1997.
- [7] D.S. Bayard, T. Kia and J. Van Cleve, "Reconfigurable Pointing Control for High Resolution Space Spectroscopy," Proc. NASA University Research Centers (URC) Technical Conference on Education, Aeronautics, Space, Autonomy, Earth, and Environment, Albuquerque, NM, February 16-19, 1997.
- [8] D.S. Bayard, "Fast Observers for Spacecraft Pointing Control," Proc. 37th IEEE Conference on Decision & Control, pp. 4202-4207, Tampa, FL, December 1998; more details in: D.S. Bayard, Internal Document JPL D-15643, March 13, 1998.
- [9] D.S. Bayard, "Autonomous Pointing Control Alignment Calibration Filter for SIRTf," JPL, Internal Document, EM 3455-99-02, April 9, 1999.
- [10] D.S. Bayard and B.H. Kang, "Instrument Pointing Frame (IPF) Kalman Filter Algorithm," JPL Internal Document, D-24809, June 30, 2003.
- [11] A. Ahmed and S. Sirlin, Gyro Calibration Filter, presentation package to SIRTf Gyro Calibration Meeting, January 27, 1999.
- [12] Bill Clark (Ed.), "SIRTf Pointing Control Subsystem Critical Design Review," Lockheed Martin Missiles and Space, Sunnyvale CA, August 7, 1998.
- [13] D.S. Bayard, A. Ahmed, and P. Brugarolas, "SIRTf Pointing History Engine (PHE)" JPL Internal Document, D-24808, June 30, 2003.
- [14] D.S. Bayard and B.H. Kang, "A High-Order Kalman Filter for Calibration of NASA's Space Infrared Telescope Facility (SIRTf)," AIAA Guidance, Navigation, and Control Conference, Paper # AIAA 2003-5824, Austin, TX, August 11-14, 2003.
- [15] D.S. Bayard, P.B. Brugarolas, D. Boussalis and B.H. Kang, "Focal Plane Survey Final Report for the Spitzer Space Telescope," JPL Internal Document, D-27667, January 30, 2004.
- [16] A.K. Mainzer, E.T. Young, L.W. Huff, and D.S. Swanson, "Pre-launch Performance Testing of the Pointing Calibration & Reference Sensor for SIRTf," IR Space Telescopes and Instruments. Edited by John C. Mather. Proceedings of the SPIE, Volume 4850. pp. 122-129, 2003.
- [17] R.W.H. Van Bezooijen, "SIRTf Autonomous Star Tracker," IR Space Telescopes and Instruments. Edited by John C. Mather. Proceedings of the SPIE, Volume 4850, pp. 108-121, 2003.
- [18] D.B. Gallagher, W.R. Irace, M.W. Werner, "Development of the Space Infrared Telescope Facility (SIRTf), IR Space Telescopes and Instruments. Edited by John C. Mather. Proceedings of the SPIE, Volume 4850. pp. 17-29, 2003.
- [19] J.P. Schwenker, B.R. Brandl, W. Burmester, J. Hora, A.K. Mainzer, P.C. Quigley, J. Van Cleve, "SIRTf_CTA optical performance test," IR Space Telescopes and Instruments. Edited by John C. Mather. Proceedings of the SPIE, Volume 4850. pp. 304-317, 2003.
- [20] J.P. Schwenker, B.R. Brandl, W.F. Hoffman, J. Hora, A.K. Mainzer, J.E. Mentzell, J. Van Cleve, "SIRTf_CTA optical performance test results," IR Space Telescopes and Instruments. Edited by John C. Mather. Proceedings of the SPIE, Volume 4850. pp. 30-41, 2003.
- [21] C. Voth, "SIRTf Pointing Performance Observer Test Results – Inertial Pointing Stability", Internal Document, SIRTf EM SESMO-03-0032, January 21, 2004.